Analyzing Multi-microgrid with Stochastic Uncertainties Including Optimal PV Allocation

H. Keshtkar, J. Solanki and S. Khushalani Solanki

Department of Electrical Engineering, West Virginia University, PO Box 6070, Morgantown, WV 26505, U.S.A.

Abstract: This paper presents the effects of Photovoltaic (PV) location on losses of the distribution system. The optimal location of PV is determined by using Particle Swarm Optimization (PSO) implemented in MATLAB-OpenDSS environment. IEEE 34-node test feeder is employed to verify the feasibility and effectiveness of the developed method. Once the optimal location is determined the challenge still remains due to the uncertain behavior of the PV system. This effect along with other stochastic behaviors such as the uncertain output power of loads like Plug-in Hybrid Electric Vehicles (PHEVs) due to their stochastic charging and discharging, that of a wind generation unit due to the stochastic wind speed, and that of a solar generating source due to the stochastic illumination intensity, add problems like frequency oscillations in a microgrid. Hence, frequency control of a multi microgrid system is also addressed.

1 INTRODUCTION

Electric energy is produced in large power plants and transmitted through High Voltage (HV) transmission systems to be distributed to consumers through Low Voltage (LV) distribution networks. Distribution system dynamics are changing with the siting of electricity generation closer to the loads and these are called Distributed Generation (DG) units (Mohammadi, 2012). These units have less environmental impact, easy siting, high efficiency, enhanced system reliability and security, improved power quality, lower operating costs due to peak shaving, and relieved transmission and distribution congestion.

However, depending on the location of DG units, some of the problems may be more pronounced and hence it is important to site the DG units to optimally exploit their potential. This paper, therefore, develops algorithms to optimally place the distributed generator considering the changing demand and generation conditions over a day. With distributed generators the distribution network can work in isolation being separated from the feeder network to form a micro-grid without affecting the transmission grid's integrity. One of the DG technologies is Photovoltaic (PV), with penetrations increasing from hundreds of kWs to MWs in LV network. Due to

these increasing penetrations in distribution systems, the utilities and planning engineers are increasingly interested in determining the best locations to place these units (Prenc, 2013).

Much of the research work on PV allocation assumes a constant generation making the problem deterministic (Medina, 2006 – Shukla 2008). For example, in (Shukla, 2008), analytical methods are presented to determine the optimal location of PV with constant generation to improve the power quality. In reality however the PV output has variations and hence an optimal location profiling the daily irradiation and energy production is necessary (Ackermann, 2001).

These units can be installed near load centers or at remote nodes to avoid large power transfers. Since distribution systems are now being operated as microgrids that form smart cities, analysis on the effects of these placements for microgrids is deemed necessary (Duenas, 2014). The problem becomes more complex with interconnection of multi-MG/smart cities with more energy layers (Guo, 2010) as compared to a single microgrid/smart city which is a passive system.

In this paper we develop an optimal PV location algorithm and analyze the effects of the PV generations and loads like PHEVs on transient stability of a multi-microgrid system. Since the

variability of a PV system can affect the findings of the optimal location a stochastic model is utilized for both PV generations and PHEV loads. Stochastic modeling and Monte Carlo simulation (MCS) are common methods to perform the stochastic optimal planning (Duenas, 2014), which have been widely used in OPF (Guo, 2010, Zhang, 2011), distribution network planning (Soroudi, 2011, Zhipeng, 2011), power market design (Sofla, 2012 – Shresta, 2008), distribution system extension planning (Kai, 2012) and microgrid energy management (Niknam, 2012). Here we utilize different models for stochastic behaviors of variable generation and demand units.

The organization of this paper is as follows: Section 2 discusses about modelling of the distribution and microgrid system. The stochastic modelling of uncertain parameters in the multi-microgrid system is also formulated in this section. PSO algorithm for optimal allocation of PV is discussed in Section 3. Section 4 describes the case studies and also presents the results of simulations. The paper is concluded in Section 5.

2 MODELING AND PROBLEM FORMULATION

We strongly encourage authors to use this document several microgrids with many DG units such as diesel, wind and solar generators integrated. In distribution systems, losses can increase operation cost and therefore it is essential to determine the optimal placement of these generators to minimize the total losses of the multi-microgrid system. Here an optimal power flow type of problem is formulated and heuristic algorithm such as particle swarm optimization is selected.

2.1 Optimization Algorithm

In this paper we will consider the placement of solar generation on $S \subset N$ nodes of multi-microgrid due to restriction imposed by distribution network operators. We assume that solar generation contribute majorly to the active power of the system thereby reducing the problem to minimization of active power losses. The methodology proposed here is described in three basic steps:

1) A constrained non-linear optimization problem is formulated to minimize the real power losses. Equality constraints related to distribution power flow equations and inequality constraints related to node voltage limits, generation capacity constraints and feeder current constraints are considered.

2) An intelligent computational technique like PSO is employed with reduced computational complexity due to reduction in search space from NPr to SPr where r are the number of PV units to be placed. Since the order of units also matters a permutations calculator rather than a combinations calculator is employed.

3) PSO is combined with three phase distribution power flow computed using backward forward sweep algorithm while the PSO globally optimizes to find the optimal DG placements and the distribution power flow determines the constraints violations. In backward forward sweep method, Kirchhoff's Current Law and Kirchhoff's Voltage Law are used to compute the bus voltage from farthest node in the backward sweep. Then in forward sweep, downstream bus voltage is updated starting from source node. The procedure stops after the mismatch of the calculated and the specified voltages at the substation is less than a convergence tolerance.

4) If the optimal values of two consecutive iterations are same with all constraints satisfied the algorithm is deemed to have converged. If not, the process continues until the criteria is satisfied.

The minimization objective function is formulated as shown in (1).

$$F = \sum_{i=1}^{N} \sum_{k=1}^{N} P_{loss_{ik}} \qquad (1)$$

Considering the conductor current $I_{ik} = \left(\frac{P_i + jQ_i}{V_i}\right)^*$ and current contribution from the solar generator as $I_i = \left(\frac{P_i}{V_i}\right)^*$, the losses of line i_k can be expressed as in (2).

$$
\begin{aligned}
P_{loss_{ik}} &= 3.\left|I_{loss_{ik}}\right|^2 .R_{ik} \\
&= 3.\left| \begin{array}{l} \left(\dfrac{P_i \cos\varphi_i + Q_i \sin\varphi_i}{\sqrt{3}V_i} - \dfrac{P_{DG_i}}{V_i^*}\right)^2 \\ + \left(\dfrac{Q_k \cos\varphi_k - P_k \sin\varphi_k}{\sqrt{3}V_k} - \dfrac{P_{DG_k}}{V_k^*}\right)^2 \end{array} \right| .R_{ik}
\end{aligned} \qquad (2)
$$

The losses over a period of one day continuously change due to changes in active power injections of the solar generation and changes in load consumption patterns. However, the location of PV once determined cannot change, so an optimal location should consider these variations in losses. The optimization algorithm is subjected to the following constraints.

(i) **Generator Rating Constraint:** Based on peak power generation, the minimum and maximum limits have been imposed on the generation capacity as

$$P_{g_i \min} \leq P_{g_i} \leq P_{g_i \max} \qquad (3)$$

(ii) **Voltage Constraint:** The optimal siting has to be obtained such that there are no bus voltages limit violations.

$$V_{\min} \leq V_i \leq V_{\max} \qquad (4)$$

(iii) **Power Balance Constraint:** The total power demand should be less than or equal to total power generation.

$$P_d \leq \sum_{i=1}^{r} P_{g_i}$$
$$Q_d \leq \sum_{i=1}^{r} Q_{g_i} \qquad (5)$$

(iv) **Feeder Current Constraint:** The feeder, current flowing through the feeder should be less than its thermal limit.

$$I_{ik} \leq I_{th_{ik}} \qquad (6)$$

An unconstrained formulation considering both objectives and constraints from (1-6) is then given in (7). Typical operations constrain the voltage to be around the nominal node voltages of the microgrid whereas the lines have to be limited to their thermal values.

$$F_x = \sum_{i=1}^{N} \sum_{k=1}^{N} P_{loss_{ik}} + \sum_{i=1}^{r} \left\{ \left\| P_{g_i} - P_d \right\|_2 \right.$$
$$\left. + \left\| Q_{g_i} - Q_d \right\|_2 \right\} + \sum_{i=1}^{N} \left\| V_i - V_i^{Nom} \right\|_2 \qquad (7)$$
$$+ \sum_{i=1}^{N} \sum_{k=1}^{N} (I_{th_{ik}} - I_{ik})^2$$

2.2 Power Flow Equations

The power balance constraints include the power flow equations that are solved iteratively and expressed as

$$V^i(i) = aV^k(i) + bI^k(i)$$
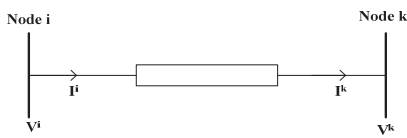$$I^i(i) = cV^k(i) + dI^k(i) \qquad (8)$$

Figure 1: Current flowing on line connecting node i and j.

The currents are those flowing on lines connecting nodes i and j as shown in Fig. 1 and a,b,c,d are matrix constants for the models of different components of the distribution network. Here loads are modelled as constant current injections, $I_s = \left(\frac{s_s(i)}{V_s(i)}\right)^*$, and

distributed generations as negative active power loads. The generators are modelled using (9) that relates the voltage u_N and the current i_N

$$u_N \overline{i}_N = s_N \left| \frac{u_N}{U_N} \right|^{\eta_N} \qquad (9)$$

where s_N is the nominal complex power and η_N is a characteristic parameter of the node N . The model (9) is called exponential model (Price, 1993) and is widely adopted in the literature on power flow analysis (Haque, 1996). Notice that s_N is the complex power that the node would inject into the grid, if the voltage at its point of connection were the nominal voltage U_N .

However, under islanded conditions the microgrids lose stability instantly and hence frequency response is of concern. The uncertain behavior of the wind generations, hybrid electric vehicles and solar generation result in frequency deviations, an analysis of which requires uncertainty models.

2.3 Uncertainty Models

The uncertainties considered in this paper include wind speed, solar radiation, and load disturbance and stochastic models for them are developed here:

2.3.1 Uncertainty of Wind Generating Units

It has been observed that wind speed deviations follow a Weibull type distribution as shown in Eq. (10) (Guo, 2010).

$$p(W,c,k) = \left(\frac{k}{c}\right)\left(\frac{W}{c}\right)^{k-1} \exp\left(-\left(\frac{W}{c}\right)^k\right) \qquad (10)$$

Where, scale factor $c = \frac{\overline{W}}{\Gamma(1+\frac{1}{k})}$ and shape factor $k = \left(\frac{\sigma}{\overline{W}}\right)^{-1.086}$, W and σ are the average value and standard deviations of wind speed, respectively, and Γ(•) is the gamma function. Using the know probability distribution function the relationship between the output power of a wind generating unit and the wind speed can be obtained and the details are provided in (Mohammadi, 2012).

2.3.2 Uncertainty of Load

Load uncertainties are twofold: those associated with

changing loads corresponding to daily consumption and those corresponding to transportation related consumption. For the daily consumption, hourly average load demand is scaled by a disturbance factor $\alpha = 1 + \delta_h$, where δ_h is the hourly disturbance coefficient and α is the disturbance factor. Both α and δ_h follow normal distribution with mean zero. Normal distribution of load can perfectly model the variable daily load in the power system $P_L = D * \alpha$ is obtained using D the hourly load data and α the disturbance factor.

The other types of loads are the Plugin hybrid electric vehicles. Since the behavior of consumers in charging their PHEVs is highly behavior dependent, three different stochastic processes for modelling PHEV are considered here.

***Brownian Motion*:** This is the continuous analog of symmetric random walk distributions, where each increment W(s+t)-W(s) is Gaussian with distribution N (0, t) and increments over disjoint intervals are independent. It is typically simulated as an approximating random walk in discrete time. Here, charging and discharging of PHEVs have been modelled by Brownian motion with sigma of 3.

***Poisson Process*:** This involves generation of random events so that: (i) arrivals occur independent of each other (ii) two or more arrivals do not occur at the same time (iii) the arrivals occur with constant intensity. Number of arrivals N (t) that occur from time zero up to time t is Poisson distributed with expected value lambda*t. The counting process N (t) is a Poisson process. The successive times between connections are Exponential (lambda) distribution. Here, arrival time of PHEVs has been modeled by Poisson process with lambda of 3.

M/M/1 Model: This is one of the random distributions (Markov process) in the category of Queuing systems. Discrete time intervals are considered so PHEV arrivals to a service center occur according to an independent sequence of a (1), a (2) …, where a (k) is the number of arrivals during time slot number k. Only one PHEV can be charged/discharged per slot (single server system). Additional PHEVs are in waiting until service is available. Therefore the number of PHEVs in the system at time k is given by

$$n(k) = n(k-1) + a(k) - 1, \quad k \geq 2$$
$$\{n(k-1) + a(k) \geq 1\} \quad\quad\quad (11)$$
$$n(1) = 0$$

This recursion defines a Markov chain n (k), k ≥1. So M/M/1 is a single server buffer model in continuous time. Considering PHEV arrivals as Poisson process

with intensity λ, an exponentially distributed random mean service time $1/\mu$ is employed for each PHEV. The resulting system size N (t) for t ≥ 0, is a Markov process in continuous time which evolves as follows: Starting from N (0) = n_0, wait an exponential time with intensity $\lambda + \mu$ (intensity λ if n_0=0), then charge with probability $\lambda/(\lambda + \mu)$ and discharge with probability $\mu/(\lambda + \mu)$. Here, number of PHEVs in the system (PHEV load size) has been modelled by M/M/1 model with λ of 1.5 and μ of 0.8.

2.3.3 Uncertainty of PV

The uncertainty of solar radiation is mainly because of the stochastic weather conditions. In this paper, cleanness index is used to model the uncertainties of weather condition. The relationship between the cleanness index and the solar irradiation can be obtained from (Srisaen, 2006). The distribution function of cleanness index can be expressed as.

$$P(k_t) = C \frac{(k_{tu} - k_t)}{k_{tu}} \exp(\lambda k_t) \quad\quad (12)$$

Where, k_t indicates the mean value of cleanness index, k_{tu} is the 0.864 theoretically, $C = \frac{\lambda^2 k_{tu}}{e^{\lambda k_{tu}} - 1 - \lambda k_{tu}}$ where $\lambda = (2\tau - 17.519 \exp(-1.3118\tau) - 1062 \exp(-5.0426\tau))/k_{tu}$ and $\tau = k_{tu}/(k_{tu} - \bar{k}_t)$.

The PV generation varies with the solar irradiation which varies according to the cleanness distribution. The relationship between the solar irradiation and the PV output power can be obtained from (Huang, 2006).

2.3.4 Load Frequency Control (LFC)

Load Frequency Control (LFC) has been implemented in the second part of the simulations for a multi-microgrid system. LFC in microgrids with nominal frequency of 50 Hz is designed to maintain frequency within 49.9 and 50.1 in normal condition by controlling tie-line flows and generator load sharing (Kroposki, 2008). The control strategy should damp the frequency oscillation in steady state and minimize them in transient state while maintaining stability.

Microgrids considered in this paper has hybrid power generation consisting of wind generators, photovoltaic, diesel generators. Power supplied to the load Ps is the sum of output power from wind turbine generators P_w, diesel generators P_g, photovoltaic generation P_{pv}, total loss power P_{Loss} and output of PHEV P_{phev} given by

$$P_s = P_w + P_g + P_{pv} + P_{loss} \pm P_{phev} \quad\quad (13)$$

Table 1: Total daily loss for different PV locations.

PV Bus	808	814	816	828	832	834	840	848	860	890
Total daily Loss (MWh)	3.8129	3.6524	3.6513	3.6182	3.4299	3.4457	3.4300	3.4294	3.4295	3.8688

LFC system in this paper uses this power flow balance equation for adjusting the frequency of the microgrid. Modeling of different parts of the system is discussed in the rest of this section.

Modeling of Wind Turbine Generator (WTG). The wind turbine is characterized by non-dimensional curves of power coefficient C_p as a function of both tip speed ratio λ and blade pitch angle β. The tip speed ratio, which is defined as the ratio of the speed at the blade tip to the wind speed, can be expressed by

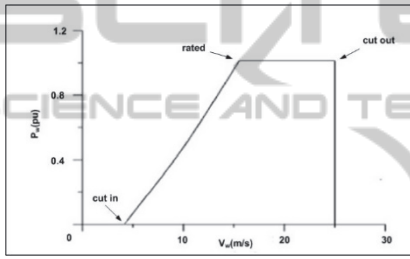$$\lambda = \frac{R_{blade}\omega_{blade}}{V_W} \qquad (14)$$

Figure 2: Characteristic curve of output mechanical power versus wind speed of the studied WTGs.

where R_{blade} (= 23.5 m) is the radius of blades and ω_{blade} (=3.14 rad/s) is the rotational speed of blades. The expression for approximating C_p as a function of λ and β is given by

$$C_p = (0.44 - 0.0167\beta)\sin\left[\frac{\pi(\lambda-3)}{15-0.3\beta}\right] - 0.0184(\lambda-3)\beta \quad (15)$$

The output mechanical power of the studied WTGs is

$$P_W = \frac{1}{2}\rho A_r C_p V_W^3 \qquad (16)$$

where, ρ (= 1.25 kg/m3) is the air density and A_r (= 1735 m2) is the swept area of blades. The characteristic curve of output mechanical power versus wind speed of the studied WTGs in this paper is shown in Fig. 2.

3 PARTICLE SWARM OPTIMIZATION (PSO)

The locations of the PV systems are optimized by

Particle Swarm Optimization (PSO) Algorithm to minimize the total losses in the system presented in (7). PSO is a multi-agent search approach, which traces its evolution to the motion of a flock of birds searching for food. It uses a number of particles that are called a swarm. Each particle traverses the search space searching for the global minimum (or maximum). In a PSO system, particles fly within a multidimensional search space. During flight, each particle sets its position based on its own experience and the experience of neighboring particles. Hence, it makes use of the best position encountered by itself and its neighbors. Similarly, the swarm direction and speed of a particle is determined by the history experience obtained by itself as well as a set of its neighboring particles (Babaei, 2009).

Each particle is a representative of PV locations that are variables that affect the total losses in each iteration. Let us consider p and s as particle position and flight speed in a search space, respectively. The best position of a particle in each step is recorded and represented as P_{best}. The best particle's index among all the particles in the group is considered as G_{best}. The convergence of PSO is ensured by use of a constriction function. Finally, the modified velocity and position of each particle can be calculated as shown in (17) and (18):

$$s_{d+1} = k*(\gamma*v_d + ac_1 rand()*(P_{best}-P_d) + ac_2*rand()*(G_{best}-P_d)) \ (17)$$

$$P_{d+1} = P_d + s_{d+1} \qquad (18)$$

Here d is the index of iteration, P_d is the current particle's position at the d-th iteration, s_d is the particle's speed of at d-th iteration, γ is inertia weight factor, ac_1 and ac_2 are acceleration constants, rand() is a uniform random value in the range [0,1], and k is the constriction factor which is a function of ac_1 and ac_2 according to (19):

$$k = \frac{2}{|2 - ac - \sqrt{ac_2 - 4ac}|} \qquad (19)$$

Where $ac = ac_1 + ac_2$ and ac>4. Appropriate choice of inertia weight, γ, makes a balance between global and local explorations. In general, γ is calculated according to (20) (Das, 2006):

$$\gamma = \gamma_{max} - \frac{\gamma_{max} - \gamma_{min}}{iter_{max}} \times iter \qquad (20)$$

Where iter$_{max}$ is the maximum number of iterations, and iter is the number of the iterations up to current stage. The iterations continue until it reaches the iter$_{max}$ or the difference between the losses calculated by best particles of the last two iterations is less than a predefined threshold.

4 CASE STUDIES AND SIMULATION RESULTS

The optimal PV locations are determined using the formulations discussed and the PSO technique. It is shown that losses are minimized under varying daily load consumptions. The PSO method described in section 3 was implemented in Matlab programming language and the unbalanced power flow solution is obtained using OpenDSS. With the placement of PVs at these optimal locations a frequency stability analysis of a multi-microgrid system is performed under stochastic load and generation behavior.

4.1 Optimal PV Allocation

As a preliminary analysis a 0.5 MW of PV generation is considered with an unknown optimal location that would result in minimum line losses. IEEE 34 node benchmark distribution system as shown in Fig 4 is considered that is inherently unbalanced with three phase cables and conductors and three phase, two phase and single phase loads. The characteristic curves of the PV are as shown in Fig. 3 (a)-(d).
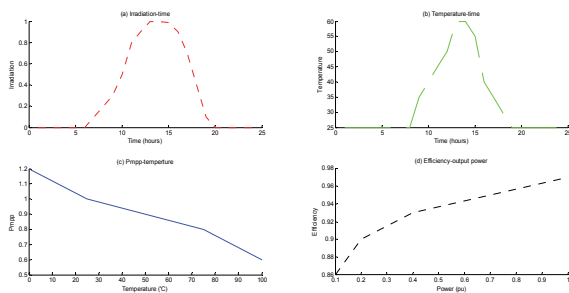

Figure 3: PV Characteristic curves; (a) Irradiation-time, (b) Temperature-time, (c) P$_{mpp}$-temperature, (d) Efficiency-power.

Initially losses are evaluated with single PV integration at node 848 of the IEEE 34 node system. Losses for an entire day are plotted as shown in Fig. 5 as the PV generation and loads vary throughout the day.

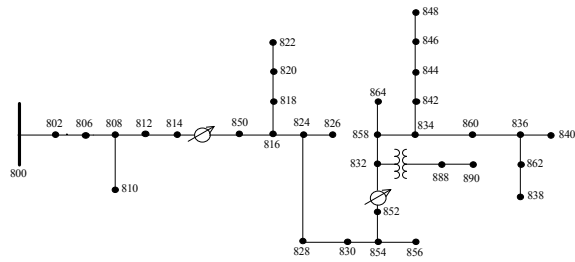The active power losses are low at night and in early morning time periods, when loading is less.

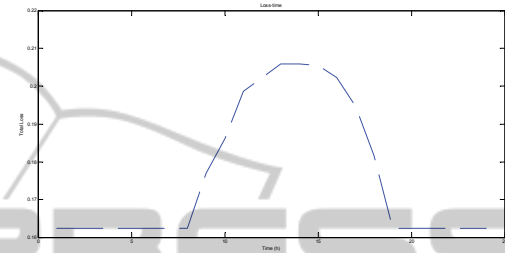Figure 4: IEEE 34 node test feeder configuration.

Figure 5: Daily losses with PV placement at node 848.

However, when the loading increases and active power generations from PV source increases, the losses increase peaking from 15:00 – 16:00 hours. Table 1 summarizes the total daily losses with PV placements at different nodes. It is seen the best location is node 848 which is located further from the main grid and close to high-demand consumers. Similar results are obtained using the developed PSO algorithm and it is seen that losses are reduced by 29% as compared to no PV installation and 13% as compared to worst PV installation.

Table 2: Total daily loss for best and worst multi-PV locations.

	Best PV locations	Worst PV locations
PV Nodes	832, 848, 860	808, 814, 890
Total daily Loss (MWh)	3.5620	3.8408

4.2 Optimal Multi-PV Allocation

Optimal locations for three PVs are obtained for IEEE 34 node test feeder by optimization algorithm (PSO) to achieve the minimum total daily losses. As seen in Table 2 the optimal node locations are 832, 848 and 860. They show 8% improvement in losses as compared to the worst locations found heuristically.

4.3 Stochastic Uncertainties in Multi-microgrid

With the determined optimal PV locations frequency

stability is evaluated considering the frequency response models and uncertainty modelling in section 2. Moreover for multiple microgrids several islands may occur simultaneously as a result of multiple contingencies in the network. PSO is adopted here to improve the frequency response by optimizing the parameters of various controllers. The details of controller design utilizing PSO for speed control are available in our prior work (Keshtkar, 2014).

Consider two similar microgrids connected through a tie line as shown in Fig. 6. This hybrid system comprises of several RES such as Wind Turbine Generator (WTG) and PV including Diesel Engine Generator (DEG) as DG that contributes to the inertia of the microgrid system. The hybrid system also includes PHEVs and other residential and small industrial loads. The PV systems are located optimally using the algorithm proposed earlier in the paper. The controllable source in this microgrid is Diesel Engine Generator whose control parameters are optimized by PSO to minimize the frequency deviations due to the disturbances. The tie line deviations of the multi-microgrid system are also considered in the objective function for optimizing controller parameters. The Area Control Error (ACE) for each microgrid considering ΔP_{tie} the tie-line power flow deviation, Δf_i the frequency deviation of each microgrid weighted by β is as shown in (21).

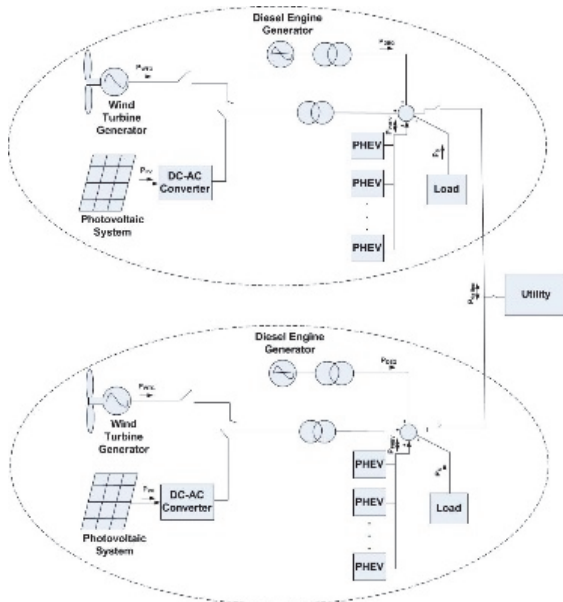$$ACE_i = \Delta P_{tie} + \beta \Delta f_i \qquad (21)$$

Figure 6: Configuration of the modeled multi-microgrid.

Three different stochastic behaviors of the PHEVs discussed in section 2 are modeled along with stochastic uncertainties of load, wind and solar generations. Frequency response of one of the microgrids of the multi-microgrid system is obtained as shown in Fig. 7. Also Fig. 8 shows the magnified frequency responses of the system in presence of different stochastic uncertainties in the multi-microgrid power system.

It is seen that stochastic modeling is essential to study the transient stability of the system and that some uncertainties can cause the frequency to severely deviate from the nominal value. For example, stochastic behavior of PHEVs creates significant overshoots in the frequency response as shown in Fig. 8 that can cause the microgrid system to be unstable. It is observed thus that a simultaneous modeling of stochastic behaviors is essential to design and test reliable and robust controllers.
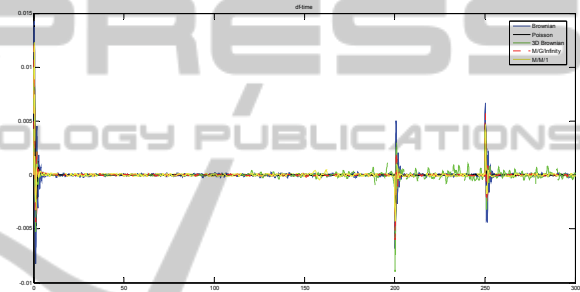

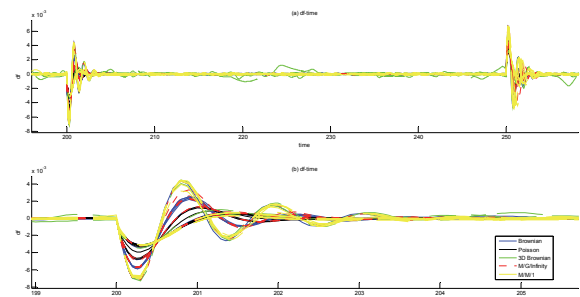Figure 7: Frequency response of one of the microgrids with different stochastic modelling.

Figure 8: Frequency response of one of the microgrids for stability margin analysis.

5 CONCLUSIONS

In this paper a method for determining the optimal placement of a PV system in distribution network based on daily power consumption/production fluctuations is described to minimize the total daily losses. The PSO optimization algorithm shows fast and accurate performance in calculating the optimal position of a PV system. Therefore, it can also serve

as a tool in calculating the optimal placement of any number and kind of DG units with a specific daily production curve such as wind turbine systems, fuel cells, microturbines with a goal of optimizing distribution power system performance.

A transient response analysis of the system with optimal PV locations and stochastic modeling of loads and generation is obtained and control parameters are designed using PSO. It is observed that simultaneous stochasticity modeling of all components should be considered for designing robust controllers.

ACKNOWLEDGEMENTS

REFERENCES

Mohammadi M., Hosseinian S.H., and Gharehpetian G.B., 2012. Optimization of Hybrid Solar Energy Sources/Wind Turbine Systems Integrated to Utility Grids as Microgrid (MG) Under Pool/Bilateral/Hybrid Electricity Market Using PSO. *Solar Energy*, vol. 86, pp. 112–125.

Prenc R., Škrlec D., Komen V. 2013. Optimal PV System Placement in a Distribution Network on the Basis of Daily Power Consumption and Production Fluctuation *EuroCon*, Zagreb, Croatia.

Medina A., Hernandez J.C., and F. Jurado, 2006. Optimal Placement and Sizing Procedure for PV Systems on Radial Distribution Systems. *International Conference on Power System Technology*.

Singh R. K., Goswami S. K. 2009. A Genetic Algorithm Based Approach for Optimal Allocation of Distributed Generations in Power Systems for Voltage Sensitive Loads. *ARPN Journal of Engineering and Applied Sciences*.

Prenc R., V. Komen, N. Bogunovi, 2012. GIS-based Determination of Optimal Accommodation of Embedded Generation on the MV Network. *International Journal of Communications Antenna and Propagation*.

Costa P. M., M. A. Matos, 2004. Loss Allocation in Distribution Networks with Embedded Generation. IEEE Transaction on Power System.

Srisaen N., and A. Sangswang, 2006. Effects of PV Grid-Connected System Location on a Distribution System. *IEEE Asia Pacific Conference on Circuits and Systems*.

Méndez V. H., J. Rivier, J. I. de la Fuente, T. Gómez, J. Arceluz, J. Marín, 2002. Impact of Distributed Generation on Distribution Losses. *In Proc. Mediterranean Power*, Athens, Greece.

Shukla T.N., S.P. Singh and K.B. Naik, 2008. Allocation of Optimal Distributed Generation using GA for Minimum System Losses. *Fifteenth National Power Systems Conference (NPSC)*, IIT Bombay.

Ackermann T., G. Andersson, L. Söder, 2001. Distributed generation: a definition. *Electric Power Systems Research*, 2001.

Duenas P., Reneses J., Barquin J., 2014. Dealing with multi-factor uncertainty in electricity markets by combining Monte Carlo simulation with spatial interpolation techniques. *IET Gener. Transm. Distrib.*

Guo L., Liu W., B. Jiao, B. Hong, C. Wang, 2010. Multi-objective stochastic optimal planning method for stand-alone microgrid system. *IET Gener. Transm. Distribution*.

Zhang, H., Li, P., 2011. Chance constrained programming for optimal power flow under uncertainty. *IEEE Trans. Power System*.

Soroudi, A., Caire, R., Hadjsaid, N., Ehsan, M., 2011. Probabilistic dynamic multi-objective model for renewable and non-renewable distributed generation planning. *IET Gener. Transm. Distribution*.

Zhipeng, L., Fushuan, W., Ledwich, G., 2011. Optimal siting and sizing of distributed generators in distribution systems considering uncertainties. *IEEE Trans. Power Delivery*.

Sofla M. A., King R., 2012. Control Method for Multi-Microgrid Systems in Smart Grid Environment - Stability, Optimization and Smart Demand participation. *IEEE PES Innovative Smart Grid Technologies (ISGT)*.

Shrestha, G.B., Pokharel, B.K., Lie, T.T., 2008. Management of price uncertainty in short-term generation planning. *IET Gener. Transm. Distribution*.

Kai Z., Agalgaonkar A.K., Muttaqi K.M., 2012. Distribution system planning with incorporating DG reactive capability and system uncertainties. *IEEE Trans. Sustain. Energy*.

Niknam, T., Golestaneh F., Malekpour A., 2012. Probabilistic energy and operation management of a microgrid containing wind/photovoltaic/fuel cell generation and energy storage devices based on point estimate method and self-adaptive gravitational search algorithm. *Energy*.

Price, W. W., Chiang, H. D., Clark, H. K., Concordia, C., Lee, D. C., Hsu, J. C., Vaahedi, E., 1993. Load representation for dynamic performance analysis. *IEEE Transactions on Power Systems*, 8(2), 472-482.

Haque M. H., 1996. Load flow solution of distribution systems with voltage dependent load models. *Elect. Pow. Syst. Res.*, vol. 36, pp. 151–156.

Huang Y., Peng F.Z., Wang J., 2006. Z-Source Inverter for Residential Photovoltaic Systems. *IEEE Trans. Power Delivery*, vol.21, no.6.

Kroposki B., Basso T., and DeBlasio R., 2008. Microgrid Standards and Technologies. *IEEE Power and Energy Society General Meeting,* pp. 1-4.

Babaei E., Galvani S. and Ahmadi Jirdehi M., 2009. Design of Robust Power System Stabilizer Based on PSO. *IEEE Symposium on Industrial Electronics and Appli-*

cations, Malaysia.

Das T.K., Venayagamoorthy G.K., 2006. Optimal Design of Power System Stabilizers Using a Small Population Based PSO. *IEEE Power Engineering Society General Meeting*.

Keshtkar, H.; Mohammadi, F.D.; Ghorbani, J.; Solanki, J.; Feliachi, A., 2014. Proposing an improved optimal LQR controller for frequency regulation of a smart microgrid in case of cyber intrusions. *IEEE 27th Canadian Conference on Electrical and Computer Engineering (CCECE)*.